Effect of Carbon Nanotube Purification on the Electrical and Mechanical Properties of Poly(ethylene terephthalate) Composites with Carbon Nanotubes in Low Concentration

Sertan Yesil,* Goknur Bayram

Department of Chemical Engineering, Middle East Technical University, Ankara 06531, Turkey

Received 18 November 2009; accepted 13 June 2010
DOI 10.1002/app.32981
Published online 29 September 2010 in Wiley Online Library (wileyonlinelibrary.com).

ABSTRACT: Surface properties of carbon nanotubes (CNTs) were altered by purification with nitric acid, sulfuric acid, ammonium hydroxide, and hydrogen peroxide. As-received and purified CNT-based conductive poly(ethylene terephthalate) composites were prepared with a twin-screw extruder. The effects of CNT purification on the surface properties of the CNTs and on the morphology and electrical and mechanical properties of CNT-based composites were investigated. Surface energy measurements showed that the acidic component of the surface energies of the CNTs increased after purification. According to Fourier transform infrared (FTIR) spectroscopy, the purification resulted in the formation of oxygen-containing functional groups on the surfaces of the CNTs. Electron spectroscopy for chemical analysis results indicate the removal of the metallic catalyst residues and an increase in the oxygen content of the CNT surfaces as a result of the purification procedure. X-ray diffraction analyses revealed a change in the crystalline structure of the CNTs after purification. All of the composites prepared with the purified CNTs had higher electrical resistivities and tensile and impact strength values than the composites based on the as-received CNTs because of the functional groups and defect sites formed on the surfaces of the CNTs during purification. © 2010 Wiley Periodicals, Inc. J Appl Polym Sci 119: 3360–3371, 2011

Key words: composites; conducting polymers; mechanical properties; surfaces

INTRODUCTION

Carbon nanotubes (CNTs) are fullerene-related structures that consist of graphene sheets rolled into cylinders that are closed at either end with caps containing pentagonal or hexagonal rings.[1] They attract great interest because of their remarkable physical properties, such as their high thermal and electrical conductivities and outstanding tensile strength. These properties make CNTs beneficial fillers for conductive polymer composite applications, such as sensors, antistatic coatings, and electromagnetic interference shielding.[2] Because their graphitic sidewalls have a low amount of defects and chemically reactive functional groups, CNTs are chemically inert, and their commercial use in polymer composites is limited because of weak interfacial interactions between the polymer matrix and CNTs. Moreover, the poor dispersion capability of CNTs in polymer composites yields undesired mechanical and electrical properties. Therefore, activation and modification of the surface of CNTs are essential for the preparation of CNT-based conductive polymer composites.[3–6]

The main aim of CNT surface treatments is to modify the surfaces of the CNTs and improve the interactions between the polymer matrix and the CNTs in the polymer composites. Enhanced interactions result in better load transfer in the composites and improve the mechanical and electrical properties.[7,8] Weak van der Waals interactions, mechanical interlocking, and covalent bonding are three main potential mechanisms of load transfer from the polymer matrix to the CNTs. Among these three mechanisms, the contributions of the first two to the load transfer are limited. However, covalent bonds between functional groups on the outer shells of CNTs and the matrix polymer have been suggested to be responsible for the observed interfacial strength between the nanotubes and the matrix in various studies.[9–11]

To increase the covalent bonding between the CNTs and the polymer matrix in composites, the surface treatment of CNTs is performed with various chemicals before the preparation of the polymer composites. The general procedure for CNT surface modification is to oxidize the CNTs with strong acids or bases (purification) first. The purpose of the

**Present address:* Department of Chemical Engineering, Kocaeli University, Kocaeli, Turkey 41380.
Correspondence to: G. Bayram (gbayram@metu.edu.tr).
Contract grant sponsor: Faculty Development Program; contract grant number: BAP-08-11-DPT2002K120510.

TABLE I
Some Physical Properties of the Components of the Composite Materials

Material	Trade name (supplier)	Specifications
PET	Melinar (Advansa, Adana, Turkey)	Melting temperature = 255°C Electrical resistivity = 10^{14} Ω cm Density = 1.4 g/cm^3
CNT	Nanocyl 7000 (Nanocyl, Sambreville, Belgium)	Average diameter = 10 nm Electrical resistivity = 10^{-4} Ω cm Surface area = 250 m^2/g

purification procedure is twofold: (1) to remove the metallic catalyst residues, which arise from CNT synthesis, and (2) to create oxygen-containing carboxyl and hydroxyl functional groups on the surfaces of the CNTs. These functional groups are the reactive sites of the CNT surfaces during further chemical modifications. They can also improve the polymer–CNT interfacial interactions.[12] After the purification step, CNTs are treated with various chemicals with different functional groups, such as silane coupling agents, ammonia, amines, surfactants, and polymeric and oligomeric materials.[13–19]

The covalent bonds of carboxyl and hydroxyl functional groups formed during purification can improve the efficiency of load transfer and dispersion in the composite. However, purification also introduces defects (dangling bonds) on the CNT surfaces and damages the crystalline structure of the CNTs. This destruction leads to a decrease in the mechanical strength and an increase in the electrical resistivity of the CNTs and affects the properties of the prepared composites.[20,21] Therefore, there should be a trade-off between the degree of CNT surface functionalization and the bulk properties of the CNTs during the purification procedure.[22,23] This balance can be achieved by optimization of the treatment period and the type and content of the purification medium.

The main aim of this study was to compare the effects of different purification methods on the properties of CNTs and poly(ethylene terephthalate) (PET)/CNT composites. For this purpose, the CNT content in the composites was kept constant at 0.5 wt %. As-received carbon nanotubes (ASCNTs) were purified with strong acids [nitric acid (HNO_3) and sulfuric acid (H_2SO_4)] and bases [ammonium hydroxide (NH_4OH) and hydrogen peroxide (H_2O_2)]. ASCNT- and purified CNT-based conductive PET composites were prepared with a twin-screw extruder (Thermo Prism, Staffordshire, UK). Apart from most of the studies in the literature, possible reasons for the differences in the structure of CNTs and composite properties were studied by means of spectroscopic and morphological characterization of the CNTs together with detailed electrical and mechanical characterization of the composites prepared with these CNTs.

EXPERIMENTAL

Materials

In this study, PET and multiwalled CNTs were used for the preparation of the composites. Some of the physical properties of these materials are shown in Table I. The CNTs were purified with HNO_3 (J. T. Baker, 65%, Deventer, The Netherlands), H_2SO_4 (J. T. Baker, 95%), NH_4OH (J. T. Baker, 30%), and H_2O_2 (J. T. Baker, 30%).

CNT purification

The ASCNTs (5 g) were added to 200 mL of purification medium. Next, the mixture was sonicated in an ultrasonic bath at 80°C. After sonication, the mixture was diluted with distilled water (1 : 5 v/v) and filtered with 0.2-μm-pore-size filter paper to recover the CNTs from the solution. The filtered CNTs were washed with excess hot and cold distilled water until no residual acid or base was present (pH of the filtrate water $>$ 5). Finally, the CNTs were dried in an oven for 24 h at 100°C. During the purification experiments, the CNTs were treated under the following eight different purification conditions. In the first part, the CNTs were sonicated in a HNO_3/H_2SO_4 mixture (1 : 3 v/v), which is the medium generally used during CNT purification in the literature, for 15 (CNT1), 30 (CNT2), 60 (CNT3), and 120 min (CNT4). In the second part, the sonication period was kept constant at 30 min, and HNO_3/H_2SO_4 mixtures (1 : 1 v/v for CNT5 and 3 : 1 v/v for CNT6) were used as the other purification medium. Finally, basic mediums (NH_4OH for CNT7 and 1 : 1 v/v NH_4OH/H_2O_2 for CNT8) were used during the 30-min purification of the CNTs.

Composite preparation and molding

During composite preparation, PET pellets were compounded with ASCNTs and purified CNTs in a Thermo Prism TSE-16-TC corotating twin-screw extruder (Staffordshire, UK) (length/diameter = 24) to obtain composites containing 0.5 wt % CNTs. The extrusion processes were performed with the temperature profile of 230–255–260–265–270°C at a screw speed of 120 rpm. Before the extrusion and

molding processes, pellets of neat PET and CNT-based PET composites were dried in a vacuum oven for 24 h at 90°C.

Specimens of composites for tensile testing and electrical conductivity measurements were prepared with injection- and compression-molding devices at 280°C. During compression molding, the samples were preheated and molded at 50 bar of oil pressure for 1.5 min and 150 bar of oil pressure for 1 min, respectively. The compression-molded samples were quenched to room temperature by tap water. Injection moldings (DSM Micro 10 cc injection-molding machine, DSM-Xplore, Geleen, The Netherlands) of the samples were performed at 15 bar of pressure at a 30°C mold temperature.

CNT and composite characterization

We determined the surface energy components[24] (total surface energy, dispersive component of the total surface energy, polar component of the total surface energy, acidic component of the polar surface energy, and basic component of the polar surface energy) of the CNTs by measuring the contact angles of the probe liquids on the surfaces of the CNTs. CNT particles were pressed as discs with 12-mm diameters under 150 bar of oil pressure, and the contact angles of the probe liquids were determined from these pressed surfaces. Diiodomethane, ethylene glycol, and formamide were used as probe liquids. Three different contact angle measurements were performed for each probe liquid, and their averages were used to calculate the surface energy components.

Fourier transform infrared (FTIR) spectroscopy (IR Prestige 21, Shimadzu, Tokyo, Japan) was used to investigate the presence of reactive groups on the surfaces of the CNTs resulting from the treatment of the CNTs with the acidic and basic purification mediums. The infrared spectra of CNTs pressed with KBr were recorded in the range 400–4000 cm^{-1}. The surface properties of the CNT samples were also analyzed by electron spectroscopy for chemical analysis (SPECS Sage HR100) with a Specs model spectrometer (SPECS Surface Nano Analysis GmbH, Berlin, Germany) (aluminum radiation at 1 W). The high-resolution spectra of oxygen (O1 s peak) were recorded with a pass energy of 48 eV under a 10^{-5}-Pa vacuum. A nonlinear background was removed from the spectra, and they were fitted with the XPSPeak41 curve-fitting program (Washington State University, Oregon, USA).

X-ray diffraction (XRD) patterns of the CNTs were obtained with a twin-tube X-ray diffractometer (100 kV Philips, PW/1050, Eindhoven, The Netherlands) that provided Cu Kα radiation (wavelength = 0.15418 nm) at 40 kV and 40 mA. The interplanar spacing between the CNT aggregates was calculated with the Bragg equation:[25]

$$n\lambda = 2d_{002}\sin\theta \quad (1)$$

where n is equal to 1 for monochromatic radiation, λ is the radiation wavelength, d_{002} is the interlayer spacing between the graphene layers, and θ is the diffraction angle of the radiation beam corresponding to Bragg's maximum. The crystallite size along the c axis (L_c) of the CNTs was calculated with the Scherrer equation:[26]

$$L_c = K\lambda/(B\cos\theta) \quad (2)$$

where K is the Scherrer constant (0.89) and B is the widening of the diffraction line measured in the middle of its maximum intensity. Further morphological analyses of the CNT samples and composites were performed with a Zeiss Supra 50 VP (Oberkochen, Germany).

The electrical resistivity values of the PET/CNT composites were measured with the two-point probe method; the probe was connected to a Keithley 2400 constant-current source meter (Ohio, USA). The volume resistivity (ρ) was calculated as follows:

$$\rho = (V/I) \times (S/L) \quad (3)$$

where V is the voltage drop, I is the current, L is the length, and S is the cross-sectional area of the sample.

The mechanical properties were investigated with a Shimadzu Autograph AG-100 KNIS MS universal tensile testing instrument according to ISO 527-2 5A standards. The tensile specimens had a thickness of 2 mm, a width of 4 mm, and a gauge length of 20 mm. According to the gauge length and the strain rate of 0.1/min, the crosshead speed of the testing instrument was selected as 2 mm/min. The impact strength of the samples were determined with a Ceast Resil Impactor 6967 impact-testing device instrumented with a 7.5-J hammer according to ASTM D 5942 (Pianezza, Italy). The impact specimens had a thickness of 4 mm, a width of 10 mm, and a length of 80 mm. Five specimens of each sample were tested, and the averages of these tests are reported with standard deviations.

RESULTS AND DISCUSSION

CNT characterization

The alteration of the surface properties and the creation of new functional groups on the surfaces of the CNTs directly changed the contact angles between the CNT surfaces and probe liquids because of the differences in the surface wettings of the CNTs by probe liquids. This change altered the surface energy components of the purified CNTs with respect to each other and compared to ASCNT (Table II). The

TABLE II
Contact Angles of Probe Liquids on the Surface of the CNT Samples and Surface Energy Components of the CNT Samples

Material code	Purification parameter	Θ_{DIM} (°)	Θ_{EG} (°)	Θ_{FORM} (°)	γ_{solid} (mN/m)	γ^d_{solid} (mN/m)	γ^p_{solid} (mN/m)	γ^A_{solid} (mN/m)	γ^B_{solid} (mN/m)
ASCNT	–	47.5	21.1	37.7	46.14	35.67	10.47	2.17	12.62
CNT1	HNO_3/H_2SO_4 (1 : 3; 15 min)	56.2	16.1	36.3	41.31	31.76	10.55	2.23	12.48
CNT2	HNO_3/H_2SO_4 (1 : 3; 30 min)	49.7	20.3	37.1	48.32	35.44	12.88	3.73	11.35
CNT3	HNO_3/H_2SO_4 (1 : 3; 60 min)	52.4	19.2	35.8	47.29	35.92	11.37	3.82	8.47
CNT4	HNO_3/H_2SO_4 (1 : 3; 120 min)	51.9	18.8	35.2	43.98	33.21	10.77	4.05	7.16
CNT5	HNO_3/H_2SO_4 (1 : 1; 30 min)	52.8	20.8	37.4	47.67	35.70	11.97	3.24	11.07
CNT6	HNO_3/H_2SO_4 (3 : 1; 30 min)	53.6	21.4	38.1	44.71	32.24	12.47	3.04	12.80
CNT7	NH_4OH (30 min)	54.8	21.8	38.5	45.04	31.56	13.48	2.23	20.38
CNT8	NH_4OH/H_2O_2 (1 : 1; 30 min)	54.1	21.7	38.0	42.23	31.96	10.27	2.29	11.53

γ_{solid} = total surface energy; γ^A_{solid} = acidic component of the polar surface energy; γ^B_{solid} = basic component of the polar surface energy; γ^d_{solid} = dispersive component of the total surface energy; γ^p_{solid} = polar component of the total surface energy; Θ_{DIM} = contact angle of diiodomethane; Θ_{EG} = contact angle of ethylene glycol; Θ_{FORM} = contact angle of formamide.

acidic component of the surface energy increased as the treatment time increased in the HNO_3/H_2SO_4 (1 : 3) mixtures (CNT1–CNT4) because of the acidic carboxyl groups formed on the surfaces of the CNTs during the acid treatment.[27] The formation of these groups was also observed in the FTIR and ESCA spectra of the CNTs. Purification for 15 min seemed to be short for the formation of new functional groups on the surfaces of the CNTs because no significant change in the polar components of the surface energy was observed for CNT1. On the other hand, the acidic component of CNT4 was nearly two times that of the ASCNTs. The total surface energy of the CNTs remained constant, whereas the basic component decreased with rising treatment time because of the growing number of oxygen-containing carboxylic acid functional groups present on the surface.[27] H_2SO_4 is a strong acid and an oxidizing agent. The main contribution to the formation of carboxyl and hydroxyl functional groups on the surface was from H_2SO_4 in the acidic mixture because the acidic component of the surface energy decreased as the H_2SO_4 concentration in the HNO_3/H_2SO_4 mixtures decreased (CNT2, CNT5, and CNT6).

After basic purification with NH_4OH (CNT7), the basic component of the surface energy increased greatly compared to that of the ASCNTs. However, purification with the NH_4OH/H_2O_2 mixture did not cause an increase in the basic component of the surface energy, and the polar component of the CNT8 was the lowest among all of the purified CNT types in this study because of the deficient sonication time for the formation of the chemical groups on the surfaces of the CNTs in the less oxidative basic purification medium. The dispersive component of the surface energy of the purified CNTs was lower than that of the ASCNTs (except for CNT3 and CNT5); this may have been due to the decrease in the effective surface area of the CNTs after the surface treatment.[24]

Figure 1 displays the FTIR spectra of the ASCNTs and purified CNTs. There were certain peaks in the FTIR spectra of all of the CNT samples, which belonged to the phonon modes of the CNTs, and these peaks were observed at the same wave number in all of the samples. As reported before in the literature, the bands at 2912 cm^{-1} were discounted as being due to CH_2 stretching and were observed in all of the CNT samples.[21] The peak at 1500 cm^{-1} was attributed to aromatic C=C stretching.[3] The peaks at 1571 and 1602 cm^{-1} were the characteristic stretching vibrations of C—C bonds related to the expected phonon modes of the CNTs.[6,21] Small peaks at 1080 and 3440 cm^{-1} indicated the presence of —OH groups on the surface, and this was an evidence for the presence of hydroxyl functional groups in the CNTs before any surface treatment.[6] A peak at 2370 cm^{-1} was also observed for all samples; this peak represented CO_2 absorption in air.[14]

Purification with strong acids and bases caused some changes in the FTIR spectra of the samples. Some new peaks appeared, and the intensities of some of the peaks increased. After purification, the presence of peaks around 1180 and 1718 cm^{-1} (corresponding to the stretching modes of the carboxylic acid groups)[28,29] and 1637 cm^{-1} [corresponding to the hydrogen-bonded carbonyl groups (C=O) that conjugated with C=C in the graphene wall][23] indicated the formation of carboxylic acid (COOH) groups on the surfaces of the CNTs. Also, the peaks around 1240, 1740, and 1427 cm^{-1} were attributed to C—N stretching vibrations,[12,15] the C=O stretching mode, and C—H bending vibrations, respectively. Under certain purification conditions, the intensities of the peaks corresponding to the carboxyl and hydroxyl groups generally became higher (CNT2–CNT5); that is, these purifications were more effective than the rest of the purification procedures in terms of the CNT surface treatment and the formation of functional groups on the surfaces of the CNTs.

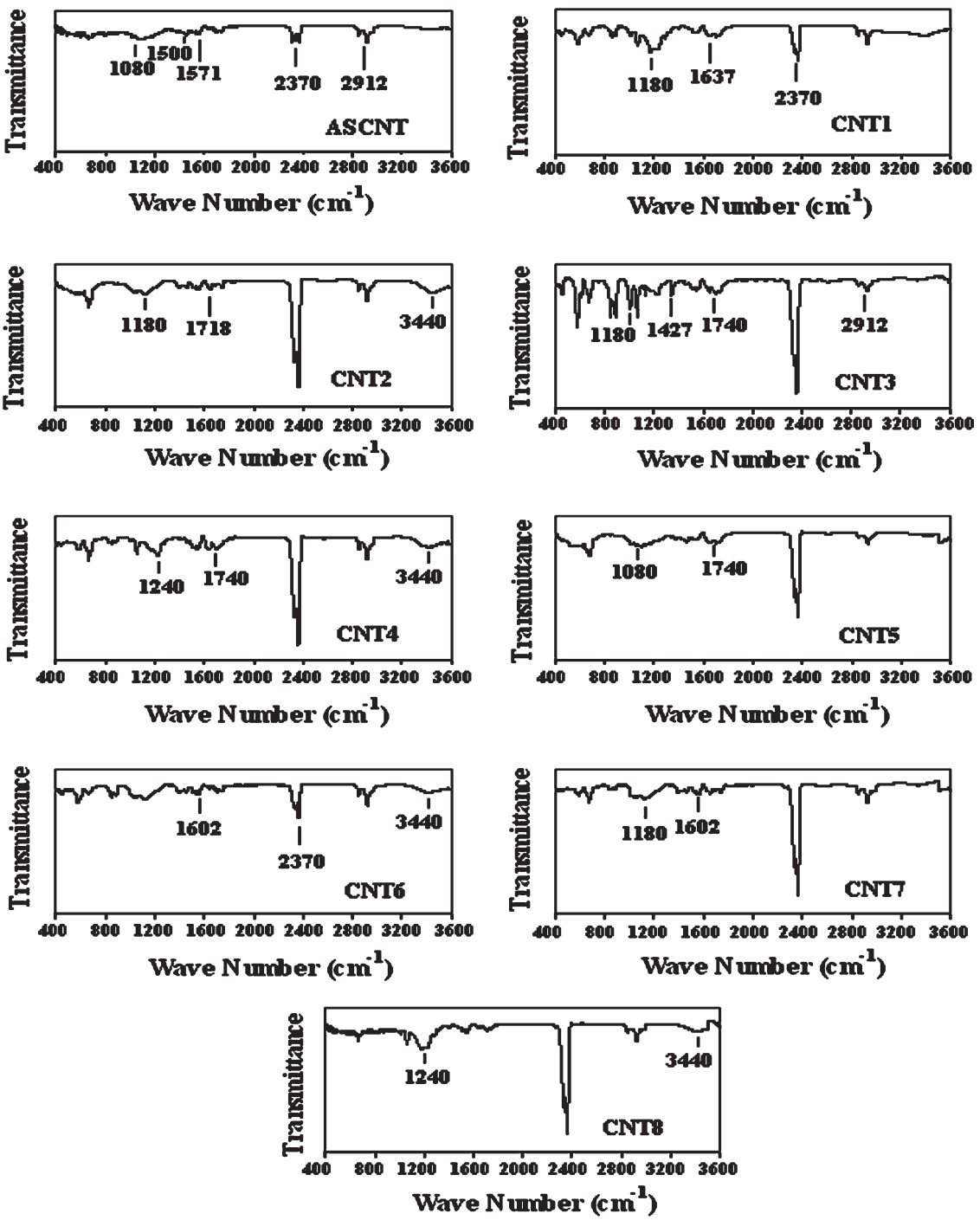

Figure 1 FTIR spectra of the CNT samples.

The ESCA spectra of the ASCNTs and purified CNTs are shown in Figure 2. The O_{1s} spectrum of the ASCNTs was fitted to two peaks corresponding to metal oxides (oxygen atoms bonded to the metallic catalyst residues present on the CNTs),[30] C=O or C—O, and to a small peak corresponding to oxygen from adsorbed H_2O; that is, a small amount of oxygen was present on the CNT surfaces in different chemical structures before any surface treatment.[31] After purification, the O_{1s} spectra of the purified CNTs were fitted to peaks for C=O, C—O, C—O—C, OH, O—C=O, C=O (esters and anhydrides), and hydroxide or carbonate bound to NH_4 types of oxygen generally; this explained the oxidation effect of the purification mediums and the formation of carboxyl and hydroxyl groups on the surfaces of the CNTs.[31–33] These functional groups were beneficial in terms of increasing the chemical compatibility between the CNTs and PET. Some of the hydroxyl groups present on the CNT surfaces might have

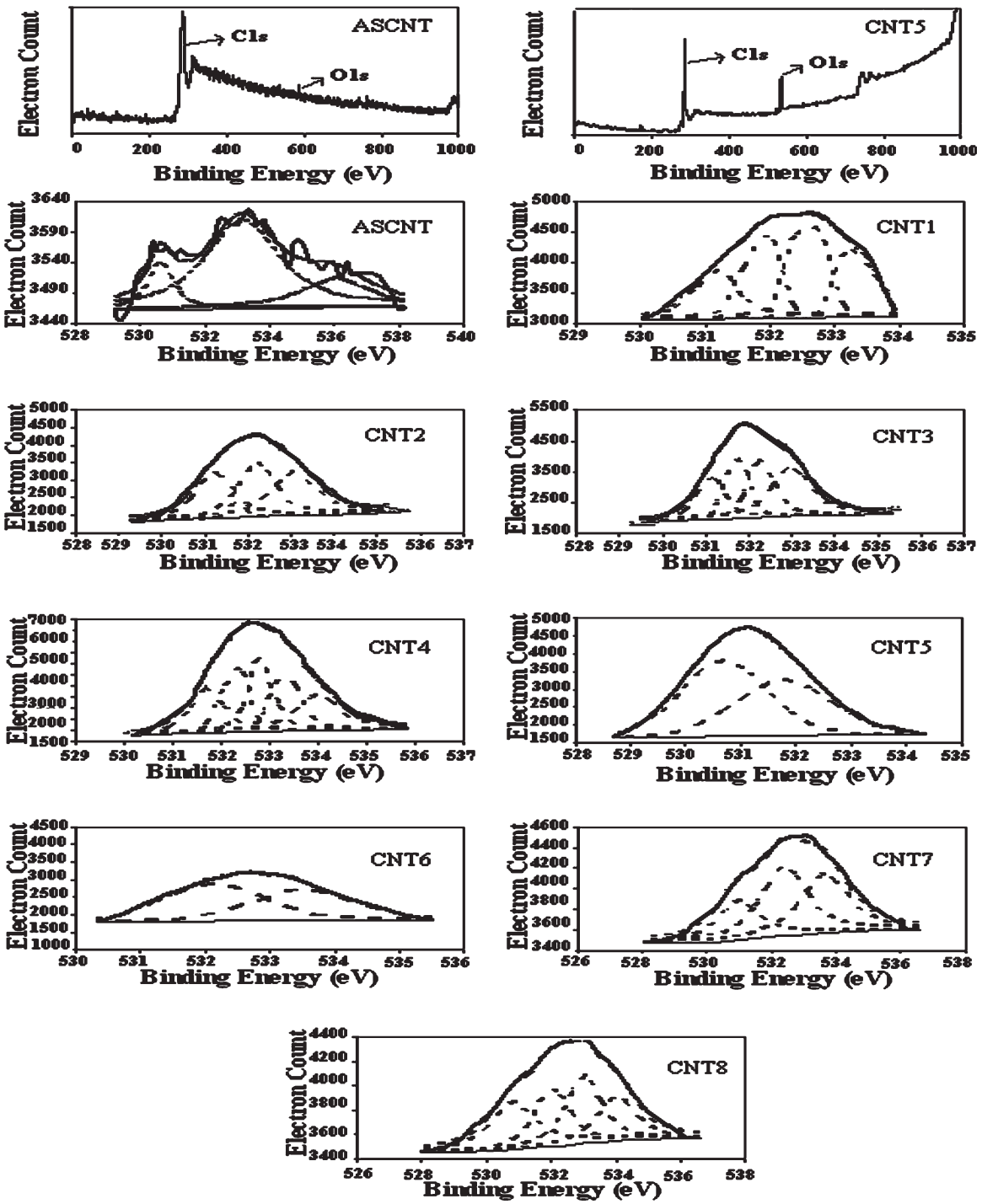

Figure 2 ESCA O_{1s} spectra of the CNT samples.

been due to water contamination resulting from the washing of the CNTs with distilled water after purification. The peaks appearing in the ESCA spectra and the chemical structures corresponding to these peaks for all of the CNT samples are explained in Table III.

The intensities (electron counts) of the peaks in the O_{1s} spectra of the purified CNT samples were higher than that of the ASCNTs; this indicated an increase in the number of oxygen-containing functional groups on the surfaces of the CNTs. This result showed that purification with acids and bases was successful in terms of the formation of hydroxyl- and carboxyl-based functional groups on the CNT surfaces.[32] Moreover, an increase in the purification duration for the 1 : 3 HNO_3/H_2SO_4 mixture resulted in an increase in the intensities of the peaks in the O_{1s} spectrum of the CNT samples

TABLE III
Peaks and Chemical Structures Corresponding to the Peaks in the ESCA O_{1s} Spectra and O/C Ratios of the CNT Samples

Material code	Peaks	O/C ratio
ASCNT	530.4 eV for oxygen bonded to the metallic catalyst residues, 532.9 eV for C=O or C—O, 535.9 eV for oxygen from adsorbed H_2O	0.03
CNT1	531.1 eV for C=O, 531.8 eV for OH, 532.6 eV for C=O or C—O, 533.4 eV for C—O—C	0.22
CNT2	531.6 eV for OH, 532.6 eV for C=O or C—O, 533.5 eV for C—O—C, 532.1 eV for C=O, O—C=O, and C=O (esters and anhydrides)	0.51
CNT3	531.8 eV for OH, 532.5 eV for C=O or C—O; 533.4 eV for C—O—C	0.54
CNT4	531.7 eV for OH, 532.8 eV for C=O, 533.4 eV for C—O—C, 534.1 eV for C—O, 532.2 eV for C=O, O—C=O, and C=O (esters and anhydrides)	0.97
CNT5	530.8 eV for hydroxide or carbonate bound to NH_4, 532.1 eV for C=O, O—C=O, and C=O (esters and anhydrides)	0.33
CNT6	532.1 eV for C=O, O—C=O, and C=O (esters and anhydrides); 533.4 eV for C—O—C	0.10
CNT7	530.8 eV for hydroxide or carbonate bound to NH_4, 533.3 eV for C—O—C, 532.1 eV for C=O, O—C=O, and C=O (esters and anhydrides)	0.06
CNT8	530.8 eV for hydroxide or carbonate bound to NH_4, 531.8 eV for OH, 532.7 eV for C=O or C—O, 533.7 eV for C—O—C	0.04

(CNT1–CNT4); this indicated that higher oxidation occurred at longer purification periods. On the other hand, any decrease in the H_2SO_4 content of the acidic purification medium (CNT2, CNT5, and CNT6) decreased the intensities of the peaks because of less effective oxidation. The carbon–nitrogen interactions that were observed in the FTIR spectra (Fig. 1) were also seen in the ESCA spectra as hydroxide or carbonate bound to NH_4.[33] This confirmed the presence of nitrogen-based chemical groups on the surfaces of the CNTs.

Basic purification resulted in the formation of oxygen-based chemical groups on the CNT surfaces to a certain extent. However, this formation was more effective in the acidic treatment than in the basic one because the intensities of the peaks in the CNT7 and CNT8 O_{1s} spectra were lower than those of the CNTs purified with acids. We calculated the oxygen-to-carbon (O/C) ratios on the surfaces of the CNT samples by taking the ratio of the areas under the O_{1s} and C_{1s} curves in the ESCA spectra for each sample;[33] these are shown in Table III. The areas under the O_{1s} and C_{1s} curves were determined by integration of the wide-scan ESCA spectra data of each CNT sample. Two representative wide-scan spectra corresponding to the ASCNT and CNT5 samples are given in Figure 2. These ratios also revealed the oxidation efficiency of the different purification conditions. The O/C ratio increased enormously with increasing treatment time for the 1 : 3 HNO_3/H_2SO_4 mixture. In addition, a decrease in the H_2SO_4 content of the acidic purification mixture resulted in a sharp decrease in the O/C ratio of the CNT samples (CNT2, CNT5, and CNT6). Basic purifications increased the O/C ratio on the surface slightly compared to the ASCNTs. Apart from the ASCNTs and CNT1, no peaks for metal oxides were observed in the ESCA spectra of the samples; this meant that the catalyst residues were removed successfully during purification.

Figure 3 shows the XRD patterns of the ASCNTs and purified CNTs. The XRD patterns of the ASCNTs and purified CNTs were similar to each other, which means that the purified CNTs had the same graphitic cylinder wall structure as the ASCNTs.[34] However, there were some changes in the crystalline structure of the CNTs after purification. The small changes in d_{002} (Table IV) of the purified CNTs did not cause a significant change in the position of the characteristic peak around 26°. Also, this peak was sharper for the ASCNTs than for the purified CNT samples (CNT2–CNT4). The change in the sharpness of this peak was due to damage in the crystalline constitution of the samples. The purification conditions, which were more

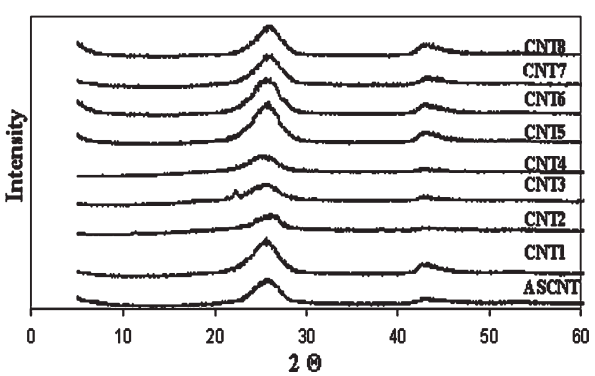

Figure 3 XRD patterns of the CNT samples.

TABLE IV
d_{002} and L_c Values of the CNT Samples

Material code	2θ (°)	B	d_{002} (Å)	L_c (Å)
ASCNT	25.98	2.74	3.43	0.51
CNT1	25.44	3.00	3.50	0.48
CNT5	25.94	2.94	3.44	0.48
CNT6	25.54	2.82	3.48	0.50
CNT7	25.72	2.77	3.46	0.49
CNT8	25.76	2.80	3.45	0.50

effective in terms of CNT oxidation, affected the crystallinity of the CNTs. As the purification period for the 1 : 3 HNO_3/H_2SO_4 mixture increased, the sharpness of the peak decreased because of the longer exposure of the CNTs to severe acidic conditions.[26] The L_c and d_{002} values were not calculated for the CNT2–CNT4 samples. The main peaks at 26° were very broad for these samples; this indicated the increase in the disordered amorphous carbon content of the CNT samples. Therefore, it did not

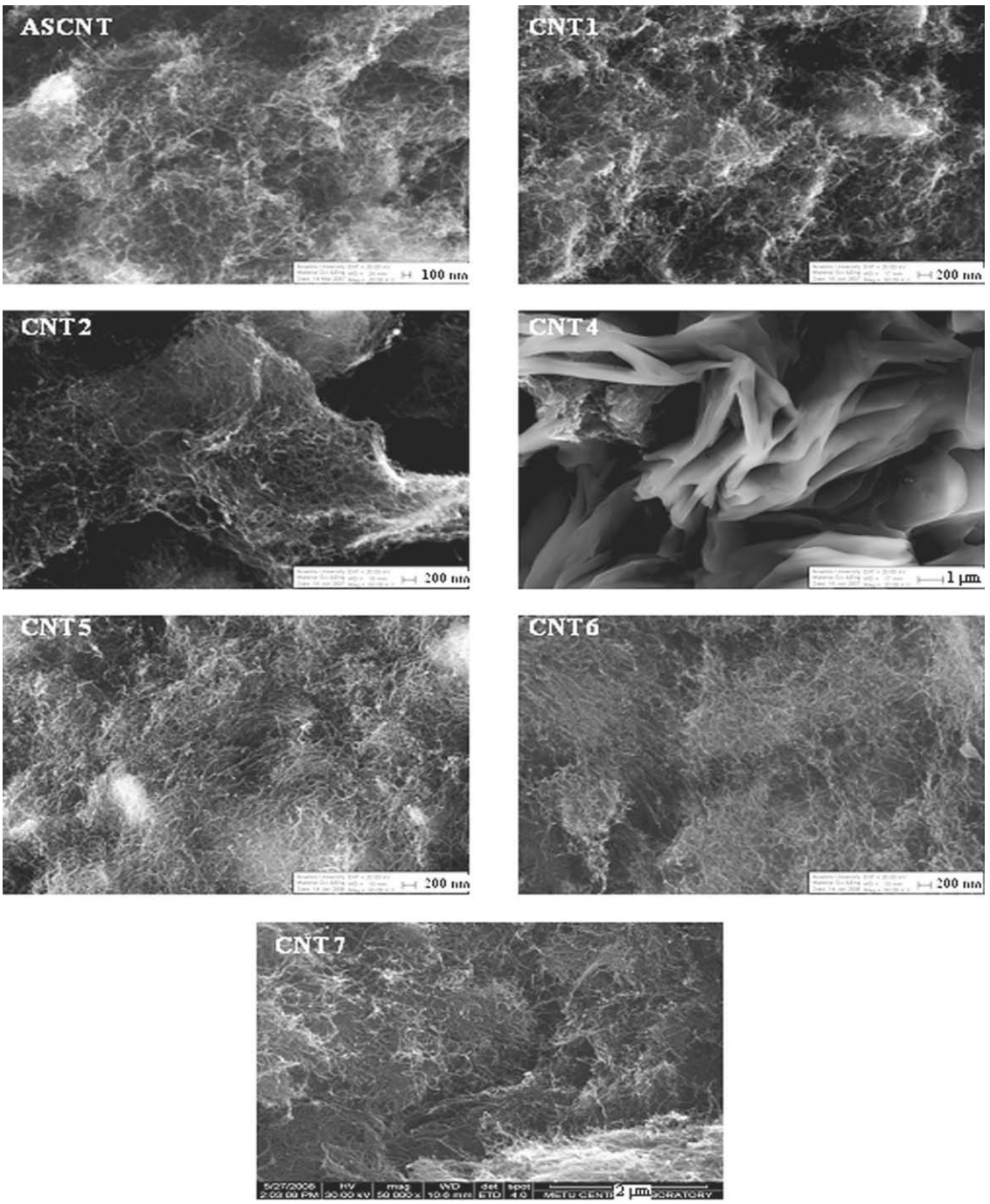

Figure 4 SEM micrographs of the CNT samples.

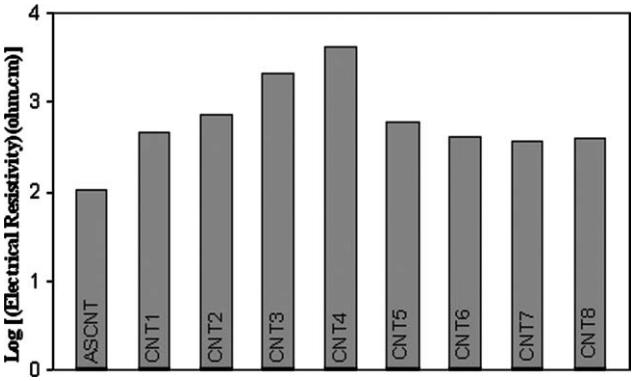

Figure 5 Electrical resistivity of the PET/CNT composites.

seem reasonable to apply the calculation methods that are used for the ordered graphitic structures to the CNT2–CNT4 samples. Because the crystalline constitution was important for the final electrical and mechanical properties of the CNTs and composites based on these CNTs,[35] there needs to be a balance between the CNT surface oxidation and the preservation of the crystalline structure. Also, purification with acidic mixtures that contains lower amounts of H_2SO_4 (CNT5 and CNT6) and bases (CNT7 and CNT8) did not cause a significant change in the crystallite size of the CNTs because of more applicable treatment conditions. The change in the structure of the CNT samples due to rough purification was also observed in the scanning electron microscopy (SEM) micrographs (Fig. 4). The micrograph of the ASCNTs showed that the CNTs randomly entangled each other in the untreated CNTs. The CNTs purified for 120 min in the 1 : 3 HNO_3/H_2SO_4 mixture (CNT4) had a more compact morphology, in which tubes were joined to each other because of the dissolution of CNT bundles in the purification medium, compared to that of the ASCNTs. On the other hand, the SEM micrographs of the other purified CNT samples resembled that of the ASCNTs.

Composite characterization

The electrical resistivity values of the PET/CNT composites are shown in Figure 5. The electrical resistivity values of all of the composites were below 10^4 Ω·cm; this confirmed that the CNT concentration (0.5 wt %) in the composites was lower than the percolation threshold concentration because the electrical resistivity values of all the composites already passed from the insulator range to the semiconductor region. At the percolation threshold, the formation of conductive CNT networks occur, and the conductive filler particles can contact each other and conduct the electrical current throughout the composite.[1]

The electrical resistivity values of the composites, including purified CNTs, were higher than that of PET/ASCNT composite. There might have been several reasons for this. After purification, the carboxyl and hydroxyl groups (Table III) present on the CNT surfaces may have increased the intrinsic electrical resistivity of the individual CNTs because of the electrically insulating oxide layer, which resulted from the oxidation of carbon-based structures. When these purified CNTs were incorporated into the polymer matrix, this insulating region on the surface limited the transportation of electrons effectively at the CNT contact points, and this increased the electrical resistivity of the composites.[12,20] The composite prepared with CNT2 had a higher electrical resistivity compared to the composites based on CNT5 and CNT6 because of more effective oxidation during purification (Fig. 2). Purification with base mixtures resulted in the lowest electrical resistivity among the composite systems based on purified CNTs because of the lower oxygen content on the surfaces of the CNTs (Table III).

Purification with strong acids degraded the crystalline structure of the CNTs, and this might have also increased the intrinsic electrical resistivity of the individual CNTs.[36] The XRD patterns of the CNT samples revealed this damage in the crystalline structure (Fig. 3), and this destruction increased the purification time in the 1 : 3 HNO_3/H_2SO_4 mixture (Table IV). As a result of these damages to the CNT structure, the electrical resistivity values of the composites based on purified CNTs increased as the chemical treatment time was increased. There was an approximately 10-fold difference between the electrical resistivity values of the PET/CNT1 and PET/CNT4 composites.

The interactions between the CNTs and PET increased after purification because of the existence of functional groups on the surfaces of the CNTs. The carboxyl and hydroxyl functional groups on the CNT surfaces could interact with the reactive end groups of PET. This might have been another reason for the increase in this electrical resistivity of the composites including purified CNTs.[37] The advanced reactivity between the CNTs and PET could have increased the wetting of the CNTs by PET and improved the dispersion of CNT particles in the polymer matrix. Conductive nanotube particles could have been surrounded by the insulating polymer matrix easily as the interaction between the filler and polymer increased. At this point, the polymer phase would have had the same function with the insulating oxide layer, and this would have increased the resistivity of the composite because it decreased the number of contact points between the conductive filler particles.[38]

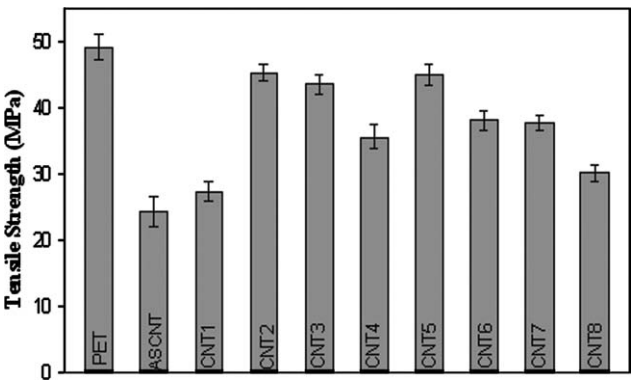

Figure 6 Tensile strength of the neat PET and PET/CNT composites.

The reinforcement effect of the CNT particles in the polymer composites depended on four main points. These were a large aspect ratio, good dispersion, alignment, and effective load transfer from the polymer to the CNTs at the interphase. Among these four main factors, the most important one for CNT reinforcement in the composites was the efficient transfer of external stresses to the CNTs.[39] In other words, the mechanical properties of the polymer composites strongly depended on the extent of the interfacial interactions between the polymer matrix and filler.

CNTs are a very strong material with an ultimate tensile strength and modulus.[40] However, PET/CNT composites generally suffer from weak mechanical properties because of their poor dispersion capabilities and interfacial adhesion of the CNTs in the polymer matrix.[41] A sharp decrease in the tensile strength value of the ASCNT-based PET composite with respect to neat PET was observed (Fig. 6). This reduction could be explained in terms of the weak interfacial adhesion between PET and the inert CNT surface, which caused debonding and pullouts of the CNTs from the surrounding matrix.[22] Also, poor dispersion and agglomeration of CNT particles in the polymer matrix, due to the incompetent shear applied during extrusion as a result of the low melt viscosity of PET, might have caused a noticeable decrease in the tensile strength. CNT addition into PET improved the tensile modulus because of the reinforcement effect of rigid fibrillar particles with a high aspect ratio (Fig. 7).[42] However, this enhancement was limited in the PET/ASCNT composite because of reasons discussed previously. The tensile strength, modulus, and impact strength values of the composites prepared with the purified CNTs were higher than those of the PET/ASCNT composite (Figs. 6–8). Oxygen-containing carboxyl and hydroxyl groups and defect sites on the surfaces of the CNTs increased the mechanical interlocking and covalent bonding between the CNTs and the PET matrix. These interactions between the composite constituents improved the efficiency of load transfer from PET to the CNTs.[41,43]

The tensile strength and modulus of the composite based on CNT2 showed a maximum, and as the sonication time was increased in the 1 : 3 HNO_3/H_2SO_4 purification medium, a decrease in these properties was observed because of the breakdown in the crystalline structure, which was observed in the X-ray and SEM analyses (Figs. 3 and 4). The PET/CNT3 and PET/CNT4 composites had lower tensile strength and modulus values compared to the CNT2 filled composite. Damages in the graphitic wall structure of the CNTs decreased the bulk mechanical properties. These directly affected the tensile and impact properties of the polymer composites.[39] Moreover, any decrease in the H_2SO_4 concentration of the acidic purification mixture caused slight reductions in the tensile strength and modulus values of the composites. The oxygen content on the surfaces of the CNTs were higher for CNT2 (Table III), but the damage in the crystalline structure was lower for CNT5 (Table IV). These two factors balanced each other, and similar

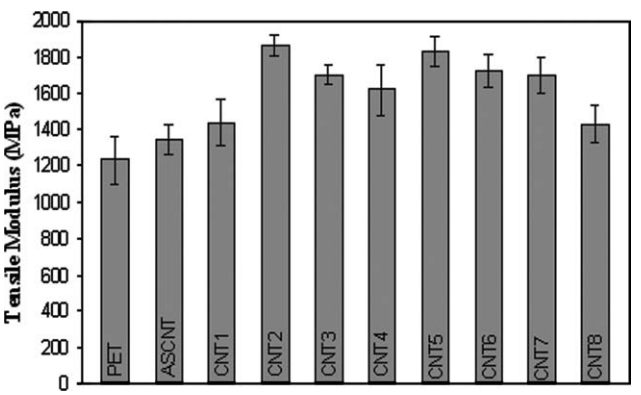

Figure 7 Tensile modulus of the neat PET and PET/CNT composites.

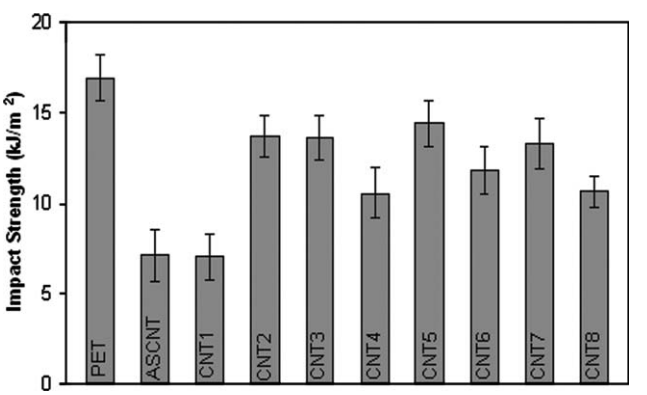

Figure 8 Impact strength of the neat PET and PET/CNT composites.

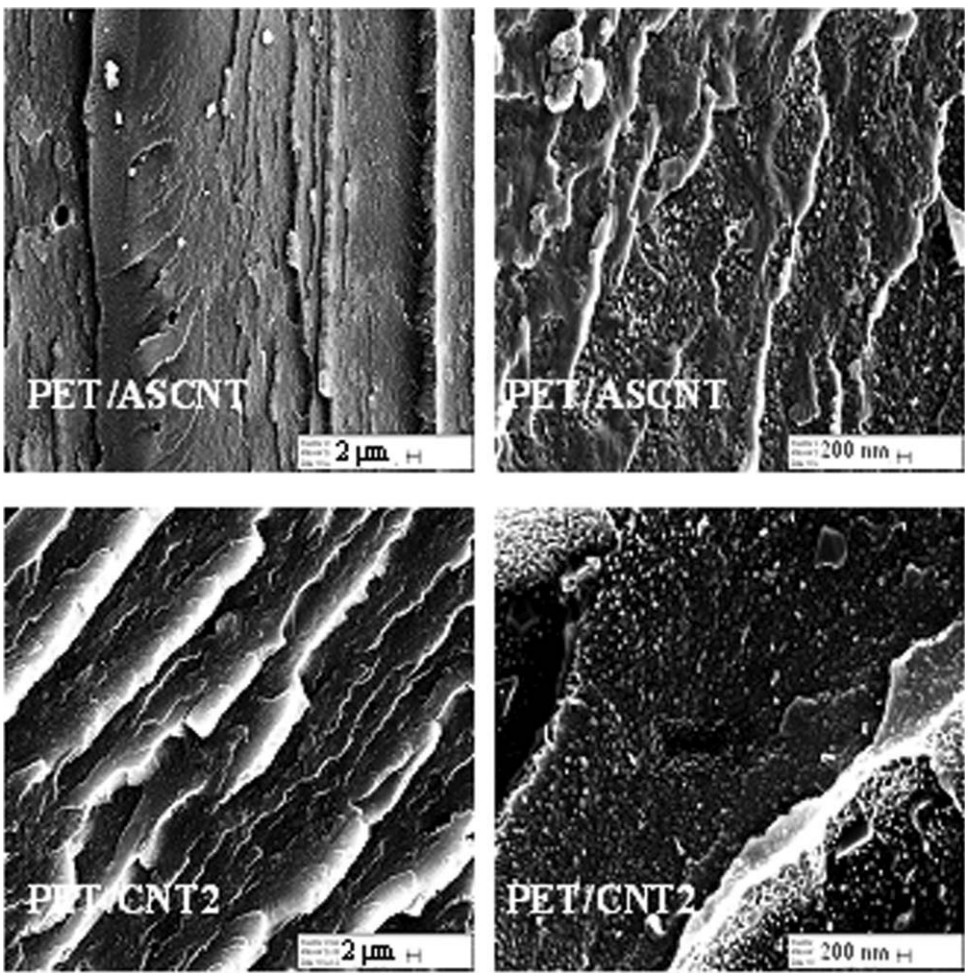

Figure 9 SEM micrographs of the PET/ASCNT and PET/CNT2 composites.

mechanical properties (e.g., tensile and impact strengths) were observed for the PET/CNT2 and PET/CNT5 composites. However, the CNT6-based composite had lower strength values compared to the PET/CNT2 and PET/CNT5 composites because of the lower oxygen content of the CNT surfaces (Table III). Basic purification did not improve the mechanical properties as much as acidic purification did because of the limited oxidation of the CNTs and the chemical compatibility between the composite constituents, which decreased the stress transfer in the composite.

CNT distribution and particle size played a distinct role in the determination of the electrical and mechanical properties of the composites.[42] Surface treatment helped the CNT dispersion in the composite because of the ionic repulsions between the chemical groups on the surface and better interfacial adhesion between PET and the CNTs. The composite containing the ASCNTs appeared to have less homogeneous CNT dispersion with larger CNT agglomerates observable on the fracture surface compared to the composite based on CNT2 (Fig. 9).

CONCLUSIONS

Surface energy measurements of CNT samples showed that the acidic component of the surface energy increased after purification with acids and bases. FTIR and ESCA analyses of the CNT samples indicated the formation of carboxyl, quinone, and hydroxyl functional groups on the surfaces of the CNTs after purification. Also, the ESCA analyses of purified CNTs indicated an increase in the oxygen concentration on the CNT surfaces compared to the ASCNT surfaces. This increase was higher in H_2SO_4-rich mixtures and at longer sonication times. The crystallite constitution of the CNTs changed with the purification in the 1 : 3 HNO_3/H_2SO_4 mixture. The damage to the crystalline structure was limited to the use of basic purification mediums. The electrical resistivity values of the composites including the purified CNTs were higher than that of the PET/ASCNT composite, mainly because of the oxide layer present on the surfaces of the purified CNTs and the damage occurring in the graphitic wall structure of the CNTs after purification. The tensile strength,

modulus, and impact strength values of the composites increased after purification compared to the ASCNT-based composite because of the enhanced interactions between the CNTs and PET; this improved the load transfer efficiency from PET to the CNTs.

References

1. Gul, V. E. Structure and Properties of Conducting Polymer Composites; VSP: Utrecht, 1996.
2. Ebbesen, T. W. Carbon Nanotubes: Preparation and Properties; CRC: Boca Raton, FL, 1997.
3. Hsin, Y. L.; Lai, J. Y.; Hwang, K. C.; Lo, S. C.; Chen, F. R.; Kai, J. J. Carbon 2006, 44, 3328.
4. Young, S. S. Polym Eng Sci 2006, 46, 1350.
5. Yaping, Z.; Aibo, Z.; Qinghua, C.; Jiaoxia, Z.; Rongchang, N. Mater Sci Eng A 2006, 435, 145.
6. Shanmugharaj, A. M.; Bae, J. H.; Lee, K. Y.; Noh, W. H.; Lee, S. H.; Ryu, S. H. Compos Sci Technol 2007, 67, 1813.
7. Rothon, R. N. Particulate Filled Polymer Composites; Rapra Technology: Shawbury, United Kingdom, 2003.
8. Friedrich, K.; Fakirov, S.; Zhang, Z. Polymer Composites from Nano to Macro Scale; Springer: New York, 2005.
9. Gojny, F. H.; Schulte, K. Compos Sci Technol 2004, 64, 2303.
10. Gojny, F. H.; Wichmann, M. H. G.; Fiedler, B.; Schulte, K. Compos Sci Technol 2005, 65, 2300.
11. Zhang, D.; Shi, L.; Fang, J.; Li, X.; Dai, K. Mater Lett 2005, 59, 4044.
12. Kim, S. D.; Kim, J. W.; Im, J. S.; Kim, Y. H.; Lee, Y. S. J Fluorine Chem 2007, 128, 60.
13. Ma, P. C.; Kim, J. K.; Tang, B. Z. Carbon 2006, 44, 3232.
14. Aibo, Z.; Wei, L.; Ming, L.; Yaping, Z. J Reinforced Plast Compos 2009, 28, 2405.
15. Misra, A.; Tyagi, P. K.; Singh, M. K.; Misra, D. S. Diamond Relat Mater 2006, 15, 385.
16. Hill, D. E.; Lin, Y.; Rao, A. M.; Allard, L. F.; Sun, Y. P. Macromolecules 2002, 35, 9466.
17. Vaisman, L.; Marom, G.; Wagner, H. D. Adv Funct Mater 2006, 16, 357.
18. Gong, X.; Liu, J.; Baskaran, S.; Voise, R. D.; Young, J. S. Chem Mater 2000, 12, 1049.
19. Cui, S.; Canet, R.; Dere, A.; Couzi, M.; Delhaes, P. Carbon 2003, 41, 797.
20. Gojny, F. H.; Wichmann, M. H. G.; Fiedler, B.; Kinloch, I. A.; Bauhofer, W.; Windle, A. H.; Schulte, K. Polymer 2006, 47, 2036.
21. Barros, E. B.; Souza, A. G.; Lemos, V.; Filho, J. M.; Fagan, S. B.; Herbst, M. H.; Rosolen, J. M.; Luengo, J. A.; Huber, J. G. Carbon 2005, 43, 2495.
22. Gojny, F. H.; Nastalczyk, J.; Roslaniec, Z.; Schulte, K. Chem Phys Lett 2003, 370, 820.
23. Shieh, Y. T.; Liu, G. L.; Wu, H. H.; Lee, C. C. Carbon 2007, 45, 1880.
24. Koysuren, O.; Yesil, S.; Bayram, G. J Appl Polym Sci 2007, 104, 3427.
25. Endo, M.; Kim, Y. A.; Takeda, T.; Hong, S. H.; Matusita, T.; Hayashi, T.; Dresselhaus, M. S. Carbon 2001, 39, 2003.
26. Takeuchi, K. J.; Marschilok, A. C.; Lau, G. C.; Leising, L. A.; Takeuchi, E. S. J Power Sources 2006, 157, 543.
27. Park, S. J.; Seo, M. K.; Nah, C. J Colloid Interface Sci 2005, 291, 229.
28. Wu, T. M.; Lin, Y. W.; Liao, C. S. Carbon 2005, 43, 734.
29. Chen, X. H.; Chen, C. S.; Xiao, H. N.; Chen, X. H.; Li, W. H.; Xu, L. S. Carbon 2005, 43, 1800.
30. Rosenthal, D.; Ruta, M.; Schlogl, R.; Kiwi-Minsker, L. Carbon 2010, 48, 1835.
31. Gardner, S. D.; Singamsetty, C. S. K.; Booth, G. L.; He, G. R.; Pittman, C. U. Carbon 1995, 33, 587.
32. Datsyuk, V.; Kalyva, M.; Papagelis, K.; Parthenios, J.; Tasis, D.; Siokou, A.; Kallitsis, I.; Galiotis, C. Carbon 2008, 46, 833.
33. Shibagaki, K.; Motojima, S. Carbon 2000, 38, 2087.
34. Shen, J.; Huang, W.; Wu, L.; Hu, Y.; Ye, M. Mater Sci Eng A 2007, 464, 151.
35. Shen, L.; Gao, X.; Tong, Y.; Yeh, A.; Li, R.; Wu, D. J Appl Polym Sci 2008, 108, 2865.
36. Kim, Y. J.; Shin, T. S.; Choi, H. D.; Kwon, J. H.; Chung, Y. C.; Yoon, H. G. Carbon 2005, 43, 23.
37. Tamburi, E.; Orlanducci, S.; Terranova, M. L.; Valentini, F.; Palleschi, G.; Curulli, A.; Brunetti, F.; Passeri, D.; Alippi, A.; Rossi, M. Carbon 2005, 43, 1213.
38. Chen, J.; Ramasubramaniam, R.; Xue, C.; Liu, H. Adv Funct Mater 2006, 16, 114.
39. Coleman, J. N.; Khan, U.; Blau, W. J.; Gun'ko, Y. K. Carbon 2006, 44, 1624.
40. Xie, X. L.; Mai, Y. W.; Zhou, X. P. Mater Sci Eng Rep 2005, 49, 89.
41. Jin, S. H.; Yoon, K. H.; Park, Y. B.; Bang, D. S. J Appl Polym Sci 2008, 107, 1163.
42. Coleman, J. N.; Khan, U.; Gun'ko, Y. K. Adv Mater 2006, 18, 689.
43. Wang, M.; Pramoda, K. P.; Goh, S. H. Carbon 2006, 44, 613.